University of Pennsylvania

3D Manufacturing of Personalized Implants for Cranial Reconstruction

Michael Solomon, Kevin Hayes, Mack Pierson, Young-Hun Kim

BE 496: Bioengineering Senior Design

Dr. Michael Rizk

May 7th, 2018

Abstract

Craniofacial injuries rank among the most prevalent ailments globally. Current viable treatment options are limited in clinical efficacy due to risks of infection, insufficient bone growth, and improper geometrical fit. We propose a personalized treatment regimen for patients with craniofacial defects to provide customized polymer-based scaffolds for optimal biocompatibility, geometrical fit, and eventual bone regeneration. After obtaining CT data of model skulls with implanted defects, data was exported and a reconstructive algorithm analyzed each 2D axial slice plane. The software identified the "missing" bone region then compiled all information to a 3D matrix to be exported as an .STL file. Processing took place in a CAD workstation before files were transferred to a 3D printer. The PCL/MSN material used in printing was created then mixed within the printing extruder, producing a homogenous scaffold. SEM imaging showed that the scaffold had an average porosity of 14.91% and an average pore size of 207µm. We successfully created an algorithm that detects defects within the skull in the individual slices of varying size (6-25cm^2) and in various calvarial locations, but faced measure error within the fits of skull cross section ranging 55% - 97%. This project therefore proves successful in creating a first prototype of a streamlined treatment process for craniofacial defects. Ideally, a patient could undergo CT imaging and have a customized, implantable scaffold within a few hours that will facilitate regeneration. There is room for algorithmic improvement, and this project still requires *in-vitro* testing for drug delivery or *in-vivo* biocompatibility testing.

Introduction

Over 1.7 million new cases of traumatic brain injury (TBI) occur every year, in the United States alone (AANS, 2018). The Center for Disease Control (CDC) defines a traumatic brain injury as "a disruption in the normal function of the brain that can be caused by a bump, blow, or jolt to the head, or penetrating head injury." Unfortunately, these damages can result in severe trauma to the brain, such as concussion or intracranial hematoma, and to the skull, such as fractures that can result in hospitalization or death (CDC, 2017). Due to the immense force required to crack bone, skull fractures are often particularly traumatic and may result in injuries that the body cannot heal naturally. Therefore, a significant need exists for patients to have a solution that quickly, cheaply, and effectively fills the required skull geometry and stimulates bone growth for normal skull function.

Currently, many approved methods exist that address the need for the proper treatment of skull fractures and craniofacial defects. The widely-considered "gold standard" is the autograft, autologous bone taken from another part of the patient's body, usually the hip, which is then implanted into the skull defect for mechanical stability and biocompatibility. Autografts generally function well because they do not usually elicit immune responses, and because they result in bone regeneration to heal the defect. However, this process requires two extensive surgeries followed by significant rehabilitation to recover while also creating financial burdens for both payers and patients. Lengthy operations can additionally result in an increased risk of infection at the bone removal site. That is, current methods to maintain the integrity of the region struggle to prevent infection before the replacement structure is inserted, ultimately making the procedure undesirable (Aydin et al., 2011). Another treatment method often considered is the allograft. This process involves harvesting bone tissue samples from a tissue bank with bone

acquired from cadavers, but these samples have a much higher rate of infection and lack the necessary molecules, proteins, and cells to form an osteogenic medium that may allow bone to grow in and heal the defect (Ullrich, 2009).

Synthetic solutions for fractures and defects have been studied for decades, but they have only begun to gain clinical credibility in recent years for treating patients with TBI. Hydroxyapatite is a calcium-based compound that shares molecular similarities with bone composition, but it lacks the required mechanical strength and breaks easily during and after implantation (Aydin et al., 2011). Understandably, mechanical failure of an implantable device near the brain could come with catastrophic consequences. Other ventures into synthetic biology can be noted, as researchers have recently begun to consider the possibility of including an element of porosity in the scaffolds while simultaneously sacrificing mechanical strength. Nonetheless, providing a porous structure allows for bone adhesion to the scaffold's edges and can promote bone growth into the implant. These features can be seen in the mixture of polyethylene and silicon, which is a porous plastic that has exceptional biocompatibility and strength, but often has complications with proper fit and issues with improper ingrowth and immune rejection (Rai et al., 2014).

Despite all of the current treatment methods available on the market, there is not one solution that adequately combines bone growth, mechanical strength, personalized fit, and minimal immune rejection. A treatment with all of those features would have a profound effect on how the medical process of surgery and healing for patients with skull fractures and defects. The aforementioned process would advance how these implants can be fabricated and when they can be utilized. In the near future, a solution that provides a quick way to develop a personalized implant for a cranial defect can provide treatment for under-served populations of people who

suffer from these injuries. For example, members of the armed forces who experience cranial defects as a result of shrapnel blasts and other traumatic situations or children born with congenital craniofacial defects such as cleft palate can eventually benefit through promotion of healthy bone growth in these troublesome regions (Boyadejiev-Boyd, 2008).

To achieve the goal of overcoming the limitations of current options, we propose a patient treatment pathway for those who suffer from TBI to ensure they receive high-quality care in a reasonable amount of time. The project is designed to, using CT imaging, develop a reconstructive algorithm that can analyze the geometry of the skull and determine the 3D region that may need replacement due to bone loss. With a model scaffold built virtually, the software will then send the design to a 3D-printing platform, where a customized, biocompatible scaffold will be printed under sterile conditions for immediate surgical implantation. The scaffold will be characterized in a manner that provides structural integrity to the skull while also promoting osteogenesis. Ideally, a patient can have an implanted scaffold within hours of undergoing CT and total native bone regeneration within a matter of weeks of surgery. This process will not only save time and money for patients, hospitals, and healthcare insurers, but it will also lead to greater patient satisfaction and optimal health outcomes for the hundreds of thousands of TBI sufferers annually.

Objectives and Approach Overview

As mentioned, our proposed solution is not to simply develop a medical device, but rather to create a streamlined treatment process with the final deliverable of a personalized, implantable scaffold with sufficient mechanical strength capable of promoting individualized bone regeneration *in situ*. The process itself takes place in a matter of six steps. Initially, a patient with a craniofacial defect will undergo computed tomography (CT) scanning to procure axial slices of

the skull, optimally at a slice thickness of 0.5mm. The CT data is imported into MATLAB (MathWorks), where our reconstruction algorithm will analyze each scan on a slice-by-slice basis. This program identifies and computes the "missing" skull in each cross-section and then stacks these 2D figures into a 3-dimensional array, which resembles the final shape of the implantable scaffold. The 3D rendering is converted to a .STL file and is then exported to a CAD workstation. After 3D accuracy is confirmed through computational fit trials, the scaffold is printed with a high-resolution 3D printer using an extrusion filament of homogenous polycaprolactone (PCL, Polysciences, MW 50 kDa) and mesoporous silica nanoparticles (MSN). The porosity of MSN particles allows the scaffold to be soaked in an osteogenic medium and seeded with patient-sourced mesenchymal stem cells (MSCs) and osteoinductive macromolecules such as TGF-β. Finally, the scaffold is surgically implanted into the skull and temporarily held in place with biodegradable materials until bone regeneration begins within a matter of weeks. The end result of this pipeline process is a structurally-sound, customized scaffold that stimulates native bone regeneration while degrading at a rate that matches osteogenesis.

While developing our innovative solution, we defined a series of discrete objectives which we hoped to achieve to ensure that our design and implementation aligned with the high-quality standards required in the clinical environment. Our first objective was to create a robust MATLAB algorithm capable of reading in a stack of CT images and outputs an .STL file with the desired scaffold geometry. The second objective was to print an implant using polymer-based materials to guarantee individualized fit while also allowing for eventual biocompatibility and biodegradation. Our third and final objective was to print samples with the PCL-MSN mixture and characterize some of its properties, ensuring proper porosity and mechanical properties.

Our project offers a solution for providing patients with a more ideal implant for cranial defects. The MATLAB algorithm allows the provider to acquire a unique CT scan for each patient, to accurately find the dimensions of the specific injuries, and to export that reconstruction data to a 3D printer in an easy-to-read file for manufacturing an individualized fit. Secondly, the printable mixture of PCL and MSN can be sterilized prior to insertion, which will help to limit the chances of immune system rejection, which are seen in many allogenic or xenogenic bone implants and some synthetic reconstruction methods. Finally, printing the material itself allows for significant time savings in the treatment process while still producing a material capable of maintaining structural integrity and catering to the individualized, accurate fit. The general process of 3D-printing is not necessarily innovative, but the combination of exact, customized fit to the patient's skull geometry with a synthetic material that can promote bone growth and provide a drug release profile is extremely innovative. Compared to current treatment options, this final scaffold design has promising potential for future clinical application in patients who suffer from TBI.

Current approaches focus on either trying to optimize fit and bone growth as seen in the autograft and allograft or to optimize structural integrity, but no one solution does it all. Our solution will allow for a patient to undergo a full treatment process: from inpatient check-in to a developed scaffold ready for surgical implantation. The device will be biocompatible, as well as mechanically-acceptable, and therefore, the existing post-operative complications are likely to be mitigated by the described streamlined process.

Specifications, Design Goals, and Constraints

We decided to view our pipeline treatment process as a two-faceted procedure: computational and biological. From a computational perspective, we determined that the

MATLAB algorithm should be able to produce a reconstructed scaffold model with an accuracy of 99% when compared to the native skull. Secondly, we hoped to ensure that, upon exporting to the 3D printer, the scale of the scaffold matched that of the surrounding skull. Most importantly, we wanted to guarantee that we could acquire CT images and print the scaffold with a 3D resolution of <2mm – any greater resolution would result in compromised mechanical strength and potential failure to stimulate osteogenesis. The biological portion, which consisted of developing the PCL/MSN material and printing of the scaffold, had several specifications that would need to be physically quantified rather than through an algorithmic evaluation process. These goals to maximize safe integration and compatibility included: printing a scaffold with a measured porosity between 60% and 90%, a quantified pore size within the 250μm to 350μm range, and a compressive strength of 90MPa. All of these values were determined through literature review of scaffold-based skull regeneration which aimed to achieve a proper balance between mechanical integrity and increased porosity for additional biologics-seeding.

To understand why the above metrics were picked for the key specifications, it is important to focus on the previously described end-goals of the treatment process. The specification of accurate scaling in the reconstructed fit is self-explanatory, as we determined that any other reconstruction : actual skull ratio aside from 1:1 would be completely ineffective to treat the defect – the implant would either be too small and unable to secure properly to the skull or too large and unable to fit in the defect at all. We determined the need for a CT resolution of less than 2mm from a recent study that used multiple CT scans and statistical analysis to show that CT scans with less than 1.25mm resolution were ideal for medical reconstruction using 2D images, otherwise mechanical properties may be sacrificed (Ford and Decker, 2016). We, however, realized that we cannot control which CT scanners were available

to us for use, so decided to slightly elevate the specification to 2mm to allow for equipment constraints. Nonetheless, most modern CT scanners are equipped to obtain isotropic data in a helical formation, which results in a slice thickness of as low as 0.25mm.

Biologically speaking, one study addressed the need for porosity, or the void fraction of negative space to material, to be within the 60-90% range as that range provides the optimal room for bone growth to infiltrate the scaffold (Roohani-Esfahani et al., 2016). Too low of a porosity results in not enough in growth and limited healing, and too high of a porosity results in not enough implant to provide adequate support prior to bone growth but 60-90% is the ideal range in between both negative consequences. Pore size was clinically determined with the previously mentioned paper of porous scaffolds for bone implants which determined that an average pore size of 200μM to 350μM would provide the best balance of bone growth and mechanical strength (Roohani-Esfahani et al., 2016). Pore sizes too large result in less material and less strength to support the implant, but pore sizes that are too small begin to inhibit the ability of bone to grow into the implant after implantation into a patient. After speaking with early stakeholder and advisor Dr. Ari Brooks, we determined that the scaffold should have the mechanical strength to handle the usual loading of the skull, but does not necessarily have to match the strength of pure autologous bone. We determined that a mechanical compressive strength of 90MPa would be optimal for this type of implant because it will allow the implant to support the surrounding tissue, and it gives the added benefit of maintaining structural integrity during pre-operative handling and implantation (Roohani-Esfahani et al., 2016).

As our project progressed, we realized that some specifications were not as important as we had initially expected. For example, when looking into mechanical properties, we realized that measuring compressive strength was vastly more important than measuring tensile strength

due to the nature of potential blows to the skull. The skull is much more likely to come into contact with a compressive blow than a tensile force that pulls the skull apart. We also altered the specification to look into its pure strength rather than the associated mechanical moduli. We also addressed the specification for determining a drug release profile after 3D printing the material, but realized as the year went on that the in vitro testing for the drug release profile fell outside of our goal of proving the feasibility of printing and developing our treatment process. This specification should be looked into after developing the dry portions of the lab as a stepping stone into the wet lab portion of the project as a future step.

While most of the standard constraint categories (economical, environmental, etc.) did not impact our project, our design process was limited, in part, by manufacturability constraints. Our software worked well to develop the proper shape for our PCL/MSN mixture to print into; however, limitations on 3D printers available severely hampered the ability to print the material properly. Our project focused primarily on proving printability of the material, but during attempts to create samples, the mixture would clump and result in an uneven scaffold piece. Even with the finest printer we could find at Allevi which used the alternative printing method of a syringe injector for loading material as opposed to filament, the PCL/MSN could not print evenly. This constraint introduced issues in testing properties of the material, mainly mechanical strength as we could not prepare samples of adequate size to fit into the clamping jaws of the Instron machine.

Following constraints, any biomedical project will have to face federal regulations to prove the efficacy and safety of the device, treatment, or desired end product. Under current U.S. Food and Drug Administration classifications, our final product of the software and implant will be classified as a Class III device. This classification is for devices that directly sustain and

support human life, and have some degree of danger and unpredictability to them which in our case stems from the implantation of the implant in the patient with the intent to foster bone growth (FDA, 2017). The base compound of PCL is an FDA approved, biodegradable polymer, but the mixture of PCL and MSN and the manufacturing process of heating and 3D printing will need to go through rigorous testing before it can become fully available on the market to patients with cranial defects. Our product also has associated standards with the American Society for Testing and Materials. First, our treatment process will have to abide by ASTM F2450-10 which is the standard guide for assessing microstructure of polymeric scaffolds for use in tissue engineered medical products which is very important for our treatment and final implant because its performance depends on its microstructure (ASTM, 2010**)**. Looking towards the future, our treatment process will also have to abide by ASTM F2902-16e1, an international standard which guides the assessment of absorbable polymeric implants which will be important as ideally our implant will one day be implanted in the skull and degrade as bone grows in (ATSM, 2016). Lastly, due to the software component of our project, our project will have to fall within the confines of the Institute of Electrical and Electronics Engineers standard 3333.2.1-2015 which is the IEEE recommended practice for three-dimensional (3D) medical modeling. This standard is directly related to our MATLAB reconstruction algorithm that will take areas from 2D CT scans and convert them into a compiled 3D model of the missing volume of skull (IEEE, 2015).

Design and Testing

Design Process – Reconstruction

To begin the reconstructive efforts, we needed to first be able to identify what a craniofacial defect actually looks like when acquired through CT scans. Thus, the first step in the process was a stage of cursory image searches online for axial CT scans of the human skull – we

then downloaded several high-resolution images and began to lay out the general steps of our algorithm. However, we ran into some issues with these images due to the fact that they were simply downloaded from Google Images, so they lacked the apparent resolution and quality that was needed for high-definition reconstruction. After this initial hurdle, we began to search through the internet to find sets of publicly-available CT images of the human skull, and fortunately, we found two sets of skulls to which we could base our initial efforts. Although these skulls did not have defects, we simply wanted to begin our algorithm on these datasets in terms of (1) reading in stacks of .dicom images, (2) creating a loop through each of the images to apply our algorithm, and (3) save the files as a CAD-friendly .STL file. This stage of the design process was completed rather quickly and was particularly successful.

The next step was to, using one individual cross section with a forged defect, develop the algorithm to define and trace the inner and outer regions of the skull; this was the most timely process of the entire reconstruction phase. While going through the various codes and callback functions of the algorithm individually would be tedious, one should, nonetheless, recognize the major features of the reconstructive algorithm. In all, it works to create a map of the outer and inner border of the skull, and the area between them is filled with pixels and subtracted from the initial image to leave just the "missing" section of bone. The outer border is mapped through a function that fits a convex hull to the skull, outputting the necessary data points. The inner border of the skull was mapped through a complex function that separated the inside data points into 360 bins (corresponding to 360 degrees). It would then determine which bins were missing any data points, which led to filling in all the degrees on the inner border without a data point. At this point in the process, we were able to successfully reconstruct the missing bone in a single cross-section.

The final step of the reconstruction process was to test our coding algorithm on our own set of model skulls. We purchased three different model skulls online that were CT-safe and were deemed biologically-accurate by an advisor. With them, we manually drilled holes of various sizes (6.98cm^2, 15.81 cm^2, 30.12 cm^2), shapes, and locations within the skull. With the help of the Penn Radiology department and the staff at Penn Presbyterian Hospital, we acquired CT scans of each of the skulls and were able to import them into MATLAB to test our algorithm. We were successfully able to read in the stacks of images and reconstruct on a slice-by-slice basis. Unsurprisingly, there were some minor issues within the code, but we were able to effectively resolve these errors in a timely manner.

Design Process – Biologic

The objective of the biologic design process was to develop a 3D printed sample of PCL/MSN polymer mixture and to measure its intrinsic properties. In order to reach the end goal, several steps had to occur throughout the design process. We realized that the first step towards developing a functional PCL/MSN sample was to find the best way to mix the two materials together. This required testing multiple mixing methods to find the best output for eventually 3D printing the sample implant and to identify which printers were available. Secondly, we had to determine what weight ratio of MSN to PCL we desired to have in our mixture to meet our specifications. Third, we then had to determine a way to incorporate the desired porous structure into the 3D printed samples to align with the specifications for pore size and porosity. We had the option to either manually design the pores into the desired structure in the .STL file prior to printing, or to alter the pores using the equipment available to our group.

These design steps resulted in tradeoffs to guarantee that a final process could be created and effectively implemented. Current developments in the field of biocompatible, controlled-

release systems for macromolecules are reaching a point where growth factors and antibodies can be delivered to a targeted site. This new technology highlights the ever-increasing potential for personalized medicine, and our device hopes to add to this field. Those systems including mesoporous silica nanoparticles have shown the most promise due to the MSN properties properties – these include: a large pore volume, a specific surface area, and an optimal pore size (Bhattacharyya et al. 2012). Furthermore, recent studies have demonstrated that the silica material in which the pore surface is coated can serve as "gatekeepers" to regulate the release of large molecules via external stimuli (Bhattacharyya et al. 2012). Due to this customizability, we fabricated these active MSN materials in collaboration with the Ducheyne Lab using a protocol they had designed in previous research efforts. The particles were then crushed into a fine powder before being mixed with PCL pellets at a ratio of 1:10. PCL was selected as the main material for the scaffold due to its biocompatibility, FDA-approval for use in clinical settings, and wide application in bone regeneration studies.

Given the non-filament nature of the material, we faced a significant shortage of available 3D printers to create our scaffolds, as the devices provided on campus required strands of specific diameters and lacked the necessary extrusion technology for the scaffold. In order to achieve our goal, we collaborated with Allevi to use their Allevi-2 printer, which has a heating syringe capable of melting the PCL and uniformly distributing the MSN before extruding through a needle. With this device, we printed scaffolds with hexagonal cross sections to examine physical and surface properties with an Instron and SEM. Although it was the best available option on our short time frame, we faced a tradeoff of quality due to the bulky nature of the needle tip and reduced accuracy of the software. Additionally, due to the limited access to the printers and long printing times, only a few samples were obtained.

Design Solutions – Reconstruction

After the reconstructive algorithm was clearly defined for the skull, and the reconstructed files were exported as .STL files, we were to run our evaluation portion of the design process. The evaluations of this algorithm all took place in SolidWorks after we were able to import both the raw skull data and the exported reconstructive data from MATLAB. As seen in **Figure 1**, the evaluation of the skull was separated into various sagittal views, comparing differences in the perceived actual skull that should be in place (pink) and the reconstructed imagery of the skull (blue). The "actual" data sets were created by simply connecting the outermost points of the known bone through a local parabolic fit. From this point, we were able to examine the error between the algorithmic data points and the perceived "actual" data points. While error ranges varied between skulls and within various cross sections in the same skull, we were generally satisfied with these initial results stemming from accuracies in range of 60% to almost 95%. Worst-case cross-sections were identified for each of the skulls. These performance results are summarized in **Table 1**. From this table, it becomes clear that the missing material is a larger problem for our software than reconstructing excess material.

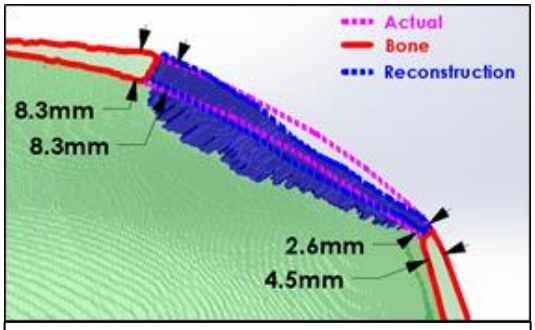

Figure 1: Virtual, cross-sectional evaluation

	Average Accuracy	Max Pos. Clearance	Max Neg. Clearance	Excess Material Err.	Missing Material Err.
Skull 1	94.6%	1.5mm	3.0mm	2.0%	5.9%
Skull 2	67.3%	1.3mm	4.8mm	11.7%	21.0%
Skull 3	63.1%	2.6mm	10.6mm	2.6%	34.2%

Table 1: Accuracy Data

Once we were satisfied with our project evaluation in the virtual space, we moved onto evaluating in the physical space. Specifically, we 3D-printed personalized implants with

polylactic acid (PLA) filament for each of the three model skulls, then visually inspected the quality-of-fit between the printed part and the skull. Visual inspection showed us that the algorithm effectively generates quality, personalized implants for skulls with a variety of defect sizes and locations. An example of these physical evaluation models can be observed with the blue PLA scaffold in **Figure 8.**

These evaluation methods proved valuable in assessing the potential real-world application of the reconstruction algorithm. Evidently, the code does need more work, as many of the cross-sectional reconstructions were convex in nature rather than concave. Although not initially expressed as a design goal, we hoped to err in the shape of concavity; doing so would sacrifice compressional and tensile strength, but it would result in less pressure put on the brain and scalp. Excess intracranial pressure may lead to serious complications upon scaffold implantation including clotting, seizures, stroke, neurological damage, or even death (Frank, 1995). With these evaluation processes, we have attempted to modify the algorithm to add a safety factor for added concavity in the design. While most of the newly printed scaffolds have a near-flush fit on the outside of the skull, we still must work on creating a more flush appearance on the inner border of the skull. This process may require altering our current coding methodology to add concave curvature to the inner border of the skull rather than somewhat linearly connecting points on the inner border. Nonetheless, the evaluation methods proved promising, but showed that the reconstruction algorithm is not precisely safe enough for human implantation at this point. After evaluating our reconstruction software in the virtual and physical spaces, we have identified several areas where our project can be improved. However, we also feel that our evaluation does, in fact, prove that our reconstruction software effectively generates

personalized implants. The next phase of project evaluation involves verification of our project's capacity to 3D-print these personalized solutions with osteo-conductive, biologic material.

Design Solutions – Biologic

We ran two different methods for mixing the PCL and MSN together. The first method relied on developing a liquid solution to mix and then drying it. Three separate amounts of PCL were weighed out and placed into 5mL glass vials. Each vial of PCL had 4mL of chloroform poured in, a stir bar was added, and each vial was placed on an individual hot plate which resulted in a solution of dissolved PCL and chloroform. Three separate amounts of MSN were added to each respective vial to produce 10%, 15%, and 20% by weight ratios of MSN to PCL. These vials were then sonicated for roughly 30 minutes, pulled out, sealed with Parafilm around the caps, and left to sit until printing. Upon opening the vials, it the chloroform took over two hours to evaporate and leave behind any sort of usable material. Heating with a hot plate in a fume hood to expedite evaporation produced brittle leftover polymer mixture, so this method had to be eliminated. We turned our focus towards a dry mixture of simply taking both the MSN and the PCL, combining them in their solid forms in a vial, and using that as our starting material. This restricted the printers available to us, so we were only able to use the bioprinters provided by Allevi, which use a pressurized, heated syringe to extrude dry polymer. The porosity of the samples was predefined in the software available for the Allevi 2 printer as 70% in addition to following a hexagonal structure as seen in **Figure 2**. Samples of strictly PCL were printed followed by samples of PCL/MSN using the dry material; however, the printer extruder struggled to uniformly extrude material and resulted in developing multiple uneven and rough samples which struggled to capture the predetermined porosity.

Figure 2: Hexagonal structure

Once the structures were 3D printed, they were SEM scanned at the Singh Center for Nanotechnology to obtain topographical data through high resolution nanoscale images. As can be seen in **Figure 3**, which shows the print at 100x magnification, the addition of MSN created visible surface alterations with the particles homogeneously distributed and well incorporated with the PCL. Zooming out to 5x magnification, as shown in **Figure 4**, the results were rather surprising. With ImageJ (FIJI), it was calculated that the average porosities were 14.91% and 32.01% while average pore sizes were 207μm and 287μm for PCL/MSN and PCL-only respectively. Given that the purpose of the MSN was to create uniformly-distributed voids for macromolecules to be loaded, it was hypothesized that the PCL/MSN mixture should have greater measured porosity. Although unexpected, these measurements could have been predicted given the nature of the 3D printer itself. When printing only PCL, the Allevi-2 had minimal difficulty extruding. But when MSN was incorporated, the printer began to "shoot" its extrusions in bursts of polymer, and the resulting filaments were thicker and less consistent. This printing patter would therefore effectively cause the pores to be smaller and less evenly distributed within the final material.

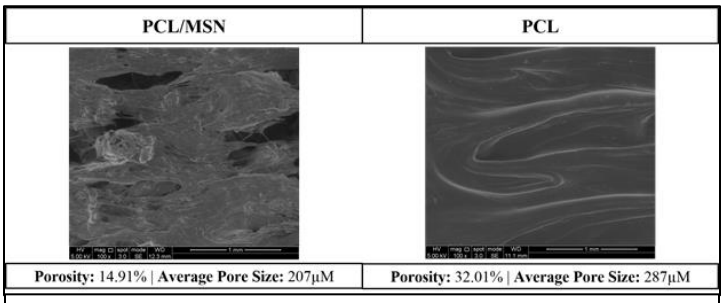

Figure 3: SEM at 100x magnification

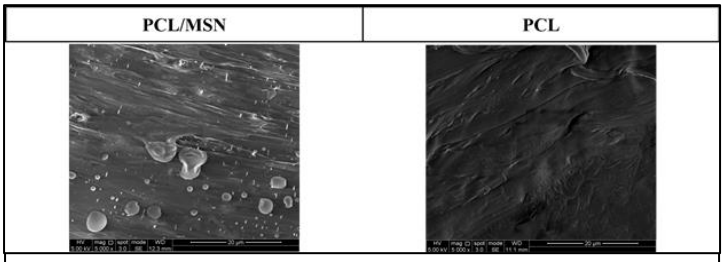

Figure 4: SEM at 5x magnification

In addition to surface properties, we attempted to evaluate the mechanical properties of the materials. With the same cylindrical structures, the Instron Test Frame (Model 5544) in the

bioengineering undergraduate lab was used to calculate tensile data. However, it was discovered that the 3 cm tall prints were not big enough for the Instron clamps to effectively latch on and pull until failure. Every PCL/MSN sample failed to obtain data, and only one PCL sample provided insight, as can be seen in **Figure 5** due to slippage of the samples out of the grip of the Instron. At approximately 65N, the majority of the ends separated from the main body before every fiber separated by 55N.

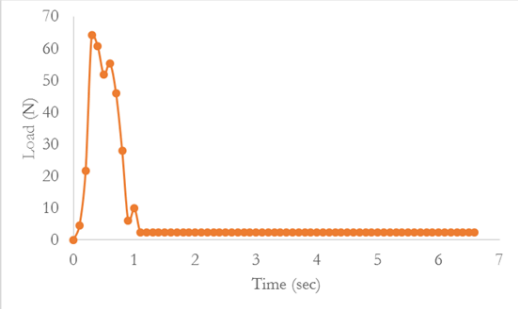

Figure 5: Instron slippage data

From these studies, it is evident that additional work is required on the biological end to ensure that the scaffold can meet the specifications related to porosity and mechanical strength. Although these results do prove to be a good initial study that demonstrates the ability to print PCL and MSN in a homogenous manner, we need to improve the 3D print quality to reach our desired porosity and cross sections. Furthermore, the test samples need to be much larger in size to perform mechanical testing, especially compressive studies. With this experience, these steps moving in the future are straightforward, and we have a strong understanding of what is required to succeed.

Optimal Design Performance and Project Impact

On a grand scale, the reconstructive aspects of this project had four major goals: (1) creating a robust algorithm for various injuries, (2) reconstructing inner and outer geometries of the skull with an accuracy of 95%, (3) scaling the scaffold to perfectly fit in the skull, and (4) create a scaffold with a 3D resolution of <2mm. We were successful in all aspects except for goal #2. As previously mentioned, three different model skulls were purchased, and defects of various sizes and locations were tested by the code. While accuracies varied slightly, there were

no errors, and the code worked in the same manner for each of the skulls in 3D space. This met specification confides us to believe it can be applied to any patient with a craniofacial defect. Secondly, the accuracy of the code still needs improvement, as discussed above. The scaling issues were quickly resolved during the data processing in SolidWorks; after loading in both the full skull and scaffold model, an aspect ratio was determined between the two to determine if, and how much, the scaffold would need to be scaled. Finally, the 3D resolution goal was met, as we were able to acquire CT images with isotropic spatial resolution (slice thickness of 0.5mm), and the 3D printing apparatus was able to print with a minimum resolution of 150 microns.

With respect to the material and biological aspect of the project, our main objectives were 1) achieve an average porosity of 60-90%, 2) have an average diameter of 200-350μm, 3) possess a compressive strength of at least 90 MPa, and 4) demonstrate ability to print PCL/MSN solutions. Unlike the reconstruction side, we had mixed results in meeting our goals as we were successful in 2 and 4. However, we are satisfied with the progress we were able to make as the targets we were unable to reach can be attributed to shortcomings in the 3D printer as discussed previously. Despite being able to create the PCL/MSN mixture at desirable ratios and the honeycomb lattice cross sections, the Allevi-2 was unable to properly print the powdery solution despite requiring many hours to attempt the print job. Therefore, we would need to create or purchase a filament extruder so that we can achieve compatibility with 3D printers available in the BME library, which have higher accuracy and finer tips.

The identified stakeholders of patients, surgeons, insurance companies, and hospital systems themselves would likely see the promise in the current design. While there is space to save money in printing less PCL with added concavity, the design process functions in a manner that efficiently produces a scaffold for various types of patients. None of these stakeholders

would likely accept the patient treatment process in its current state due to the dangers of inconsistent accuracy in the inner-geometry modelling along with unproven scaffold properties. However, with minor software improvements to meet our design goal of 95% accuracy, then the reconstruction software will prove useful and beneficial for all stakeholders. After acquiring a CT scan, the data can be exported and run into the reconstructive algorithm, which automatically designs the scaffold and saves as a CAD-friendly .STL file for printing. Additionally, testing of various PCL+MSN mixtures for both porosity and compressive strength will also tell stakeholders what to expect from the scaffold once it can be implanted. In all, the process would ideally take around three hours from beginning of the CT scan to having a printable file. With these additional increases in accuracy, the patient-treatment platform will become highly streamlined with no detriment in patient safety, scaffold strength, overall costs, or treatment time. Stakeholder confidence in the final design will also be increased significantly with more testing of the various necessary biological and mechanical properties, such as compressive strength and porosity measures.

Display of Final Protocol/Process/Project

Figure 6 shows an illustration of the final algorithm working in a single 2D slice plane. This algorithm will then fill in the area between the red lines, which will isolate the "missing" piece of bone. These reconstructions will then be compiled into three dimensional space and exported to a CAD-friendly file. This final exported image in the .STL file can be seen in **Figure 7**. From this stage, the file is then exported to a 3D printer, which, with the PCL+MSN material combination, is able to print the scaffold seen in **Figure 8**. As stated above, this scaffold has sufficient mechanical properties and biochemical release profiles. In the most general sense, these images show the major visual components of our final project and design. As mentioned, though, the goal was not to create a simply scaffold or device, but rather an entire patient treatment process, which may be difficult to display in terms of deliverable images. To see the overall goal of the project, one should consider the **Project Illustration** image and corresponding explanation.

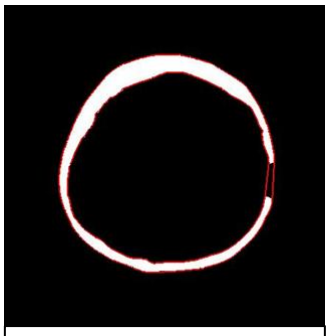

Figure 6: Reconstruction

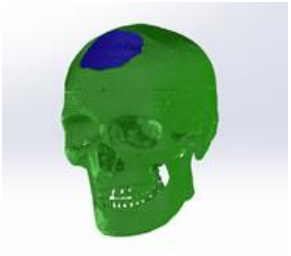

Figure 7: STL Model

Figure 8: Final fit

Project Illustration

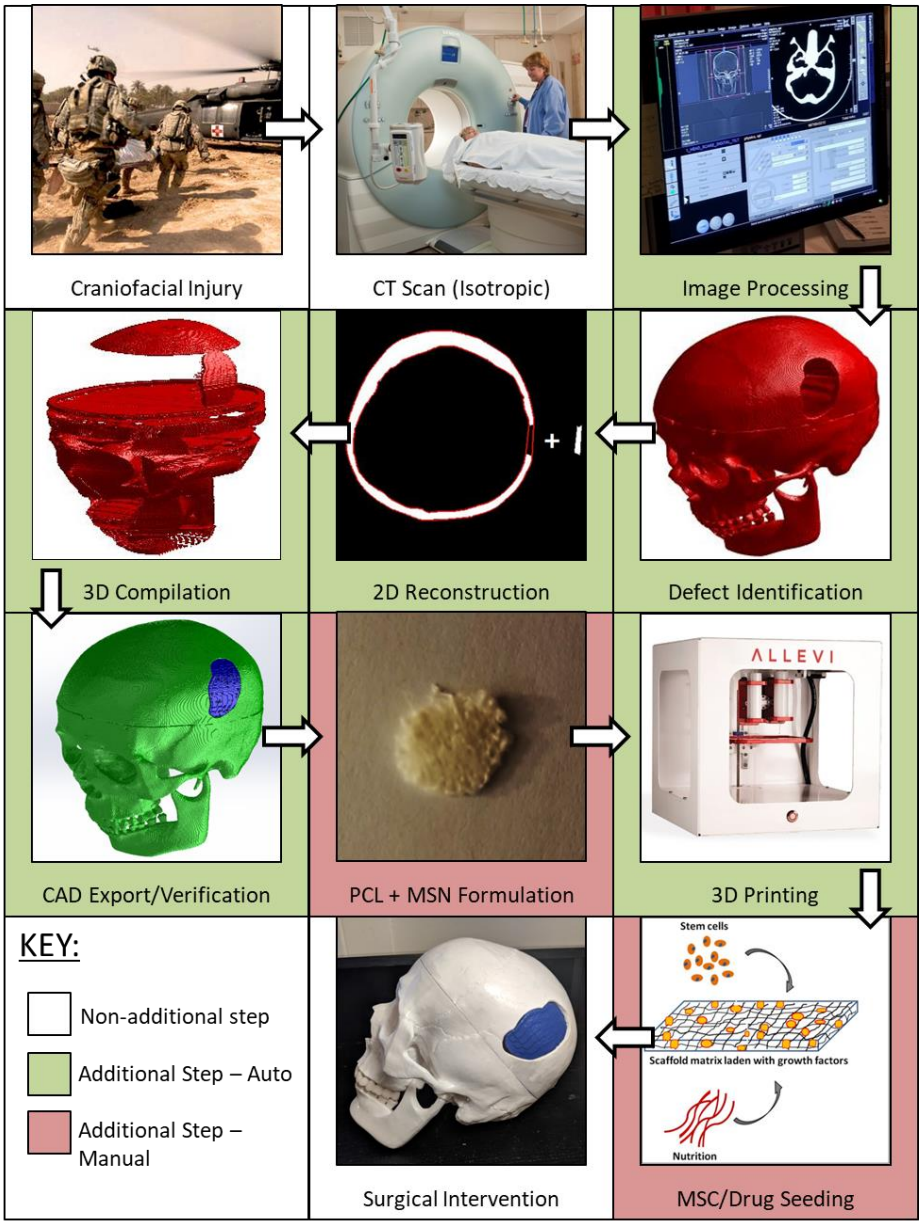

The illustration above represents our 11-step, pipelined process for generating personalized patient implants. In an ideal scenario, the patient could enter a hospital, and within three hours, he or she could be holding the scaffold that is ready to plant within their skull for the defect. That is, the algorithm only adds approximately 45 minutes to the treatment process and the 3D printing and scaffold generation takes approximately 2 hours.

Budget

We successfully managed to keep our costs under the given budget of $600, as shown in **Figure 9**. The majority of our materials were free for us, namely the use of university resources such as the Instron (Instron 4444, Instron, Norwood, MA) for mechanical testing provided by the undergraduate bioengineering lab, the 3D printers (MakerBot Replicator 5th Generation, MakerBot, Brooklyn, NY) in the Rapid Prototyping Lab for produced mock implants, and the Hospital of the University of Pennsylvania's CT scanner (Siemens Definition Flash, Siemens, Munich Germany) for procuring CT scans of our test skulls. We anticipated spending money on the scanning electron microscope imaging which is used to observe pore size and porosity. However, we were able to use Dr. Ducheyne's lab resources to secure free SEM imaging at the Singh Center for Nanotechnology (Quanta 600 FEG ESEM, FEI, Hillsboro, OR). In our initial project cost estimates, we did not anticipate the necessity for purchasing additional PCL, for $182.00, to prepare more of our PCL and MSN solution for printing samples. Lastly, we slightly underestimated the cost of three model skulls to test our MATLAB algorithm on with a projected cost of $100 and an actual cost of $121.79. Overall, the final cost of completing the project cost was $303.79, which is well under the allotted budget and can be considered a low-cost alternative to other solutions currently available with respect to preparing the implant prior to surgery.

Item	Budgeted	Actual	Use
SEM	$ 300.00	Free	Measuring porosity
Instron	Free	Free	Determining material strength
3D Printer (RPL)	Free	Free	Printing for geometrical fitting
3D Printer (Allevi)	Free	Free	Printing PCL/MSN solution
CT Scan	Free	Free	Acquiring data
Skull Models (x3)	$ 100.00	$ 121.79	Physical test for reconstruction
Bone Graft Material	Free	$ 182.00	3D printing material

Figure 9: Budget chart for the year

Conclusions and Summary

In all, we were able to successfully develop a patient-treatment pipeline for patients with craniofacial defects. This process will be able to help the ever-increasing patient population who are not optimally treated, due to the mechanical or biochemical shortcomings of current treatment modalities. As seen in the **Project Illustration**, a patient with a craniofacial injury can enter a hospital, and within a matter of hours, they can be holding their own customized scaffold. The algorithm works to reconstruct CT images on a slice-by-slice basis, and then export the scaffold to a CAD-friendly file for 3D printing. While the reconstruction process is going on, printing technicians can prepare a necessary amount of PCL+MSN solution. Then, the .STL file takes about two hours to print in full, depending on the size of the defect. From this point, the scaffold can then be loaded with mesenchymal stem cells, immunosuppressants, and various other bioactive components to promote osteogenesis when the scaffold is surgically implanted.

We were able to meet many of our reconstruction specifications including scaling accuracy and printing resolution. However, we fell short in terms of 2D cross-sectional reconstruction accuracy, especially in the mapping of the inner border of the skull. This error is likely not impossible to fix, but remains an issue that currently limits the efficacy and applicability of the treatment pipeline. In terms of the scaffold itself, we were able to observe a maximum tensile load and ultimate compressive strength within the pre-defined parameters. However, the scaffold did fall short in terms of porosity, which may affect drug release profiles. Evidently, the project is incomplete on several fronts. First, we did not have sufficient time to run any biological testing either in vitro or in vivo to determine if the drugs will release properly or if the MSCs will undergo osteodifferentiation. Secondly, the reconstructive algorithm will need to be altered to ensure greater accuracy and a more concave design of the scaffold once

reconstruction is complete. These modifications will ensure that the scaffold is safe for clinical use, which will be next major step in ensuring the effectiveness of the patient treatment pipeline.

Attributions and Acknowledgements

Our project would not have been as successful without the help, support, and guidance of the following individuals and organizations. We would like to thank our course instructor Dr. Michael Rizk for continued guidance on a weekly basis. Additionally, we are grateful for the help provided by our primary investigator Dr. Paul Ducheyne and his lab staff, including Dr. Sanjib Bhattacharyya and Dr. Pedro Alvarez-Urena. Our early medical advisor Dr. Ari Brooks was supportive in guiding us through the mindset of our clinical/surgeon stakeholder. Again, thank you to those at Allevi for letting us use their bioprinters, including employee, and our friend Gabe Montoya. We would also like to express thanks to our M&T advisor Dr. Sangeeta Vohra, Dr. Andrew Maidment and his associates Dr. Scott Cupp and Mr. Michael Colfer from Penn Medicine's Department of Radiology for this assistance in performing CT scans, Dr. Jamie Ford and the Singh Center for Nanotechnology for assisting us with performing SEM imaging on our samples, and the Towne Business Office for handling our orders and various logistics. Thank you all for your time and help.

Works Cited

1. American Association of Neurological Surgeons. (2018). Traumatic Brain Injury – Causes, Symptoms and Treatments. [online] Available at: http://www.aans.org/Patients/Neurosurgical-Conditions-and-Treatments/Traumatic-Brain-Injury
2. Centers for Disease Control and Prevention. (July 6, 2017). Traumatic Brain Injury & Concussion. [online] Available at: https://www.cdc.gov/traumaticbraininjury/index.html
3. Harvard Medical School. (January 2013). Head Injury In Adults. [online] Harvard Health. Available at: https://www.health.harvard.edu/diseases-and-conditions/head-injury-in-adults
4. Qureshi, N. and Kopell, B. (July 18, 2017). Skull Fracture Treatment & Management. [online] MedScape. Available at: https://emedicine.medscape.com/article/248108-treatment#d10
5. Aydin, Seckin et al. "Cranioplasty: Review of Materials and Techniques." Journal of Neurosciences in Rural Practice 2.2 (2011): 162–167. PMC. Available at: https://www.ncbi.nlm.nih.gov/pmc/articles/PMC3159354/
6. Ullrich, Peter F. (November 25, 2009). Allograft: Cadaver Bone From A Tissue Bank. SPINE-health. Veritas Health. Available at: https://www.spine-health.com/treatment/spinal-fusion/allograft-cadaver-bone-a-tissue-bank
7. Rai, Anshul et al. "Utility of High Density Porous Polyethylene Implants in Maxillofacial Surgery." Journal of Maxillofacial & Oral Surgery 13.1 (2014): 42–46. PMC. Available at: https://www.ncbi.nlm.nih.gov/pmc/articles/PMC3955470/

8. Boyadjiev Boyd, Simeon. (February 208). Overview Of Congenital Craniofacial Abnormalities - Pediatrics. MSD Manual Professional Edition. Merck. Available at: https://www.merckmanuals.com/professional/pediatrics/congenital-craniofacial-and-musculoskeletal-abnormalities/overview-of-congenital-craniofacial-abnormalities
9. Roohani-Esfahani, Seyed-Iman, Peter Newman, and Hala Zreiqat. "Design and fabrication of 3D printed scaffolds with a mechanical strength comparable to cortical bone to repair large bone defects." Scientific reports 6 (2016): 19468. Available at: https://www.nature.com/articles/srep19468
10. Ford, Jonathan M., and Summer J. Decker. "Computed tomography slice thickness and its effects on three-dimensional reconstruction of anatomical structures." Journal of Forensic Radiology and Imaging 4 (2016): 43-46. Available at: https://www.jofri.net/article/S2212-4780(15)30020-4/abstract
11. US Food and Drug Administration. (December 29, 2017). Learn If A Medical Device Has Been Cleared By FDA For Marketing. FDA.gov. Available at: https://www.fda.gov/MedicalDevices/ResourcesforYou/Consumers/ucm142523.htm
12. "IEEE 3333.2.1-2015 - IEEE Recommended Practice For Three-Dimensional (3D) Medical Modeling." Standards.IEEE.org. Available at: http://standards.ieee.org/findstds/standard/3333.2.1-2015.html
13. ASTM F2450-10, Standard Guide for Assessing Microstructure of Polymeric Scaffolds for Use in Tissue Engineered Medical Products, ASTM International, West Conshohocken, PA, 2010. Available at: https://www.astm.org/Standards/F2450.htm

14. ASTM F2902-16e1, Standard Guide for Assessment of Absorbable Polymeric Implants, ASTM International, West Conshohocken, PA, 2016. Available at: https://www.astm.org/Standards/F2902.htm
15. Frank, Jeffrey I. "Large hemispheric infarction, deterioration, and intracranial pressure." *Neurology* 45.7 (1995): 1286-1290.
16. Bhattacharyya, Sanjib, Henson Wang, and Paul Ducheyne. "Polymer-coated mesoporous silica nanoparticles for the controlled release of macromolecules." Acta biomaterialia 8.9 (2012): 3429-3435.